Protein Science (2000), *9*:2200–2209. Cambridge University Press. Printed in the USA.

Three-dimensional model of the extracellular domain of the type 4a metabotropic glutamate receptor: New insights into the activation process

ANNE-SOPHIE BESSIS,[1] HUGUES-OLIVIER BERTRAND,[2] THIERRY GALVEZ,[3] CYRIL DE COLLE,[3] JEAN-PHILIPPE PIN,[3] AND FRANCINE ACHER[1]

[1]Laboratoire de Chimie et Biochimie Pharmacologiques et Toxicologiques, UMR8601-CNRS, Université René Descartes-Paris V, 75270 Paris Cedex 06, France
[2]Molecular Simulations Inc., Parc Club Orsay Université, 91893 Orsay Cedex, France
[3]Centre INSERM-CNRS de Pharmacologie-Endocrinologie, UPR 9023-CNRS, 34094 Montpellier Cedex 5, France

(RECEIVED June 13, 2000; FINAL REVISION September 8, 2000; ACCEPTED September 18, 2000)

Abstract

Metabotropic glutamate receptors (mGluRs) belong to the family 3 of G-protein-coupled receptors. On these proteins, agonist binding on the extracellular domain leads to conformational changes in the 7-transmembrane domains required for G-protein activation. To elucidate the structural features that might be responsible for such an activation mechanism, we have generated models of the amino terminal domain (ATD) of type 4 mGluR ($mGlu_4R$). The fold recognition search allowed the identification of three hits with a low sequence identity, but with high secondary structure conservation: leucine isoleucine valine-binding protein (LIVBP) and leucine-binding protein (LBP) as already known, and acetamide-binding protein (AmiC). These proteins are characterized by a bilobate structure in an open state for LIVBP/LBP and a closed state for AmiC, with ligand binding in the cleft. Models for both open and closed forms of $mGlu_4R$ ATD have been generated. ACPT-I (1-aminocyclopentane 1,3,4-tricarboxylic acid), a selective agonist, has been docked in the two models. In the open form, ACPT-I is only bound to lobe I through interactions with Lys74, Arg78, Ser159, and Thr182. In the closed form, ACPT-I is trapped between both lobes with additional binding to Tyr230, Asp312, Ser313, and Lys317 from lobe II. These results support the hypothesis that mGluR agonists bind a closed form of the ATDs, suggesting that such a conformation of the binding domain corresponds to the active conformation.

Keywords: ACPT; docking; homology modeling; metabotropic glutamate receptors

Elucidating the activation mechanism of G-protein coupled receptors (GPCR) is a major issue. In the case of most rhodopsin-like (family 1, see Bockaert & Pin, 1999) GPCRs, the agonists interact in a cavity within the 7-transmembrane domain (TM), and stabilize the active conformation (Bockaert & Pin, 1999). In the case of family 3 GPCRs, the agonist binding site is located within their large extracellular domain (Conn & Pin, 1997; Pin et al., 1999), whereas the G-protein activation is still mediated by the intracellular loops of their 7TM domain (Pin et al., 1994; Gomeza et al., 1996). It is actually not known how the agonist binding on the extracellular domain of these family 3 GPCRs leads to the conformational changes required for G-protein activation (Pin et al., 1999).

This family 3 of GPCRs encompasses the metabotropic glutamate receptors (mGluR), the $GABA_B$ receptor, a calcium-sensing receptor, several putative pheromones receptors and a taste receptor (Bockaert & Pin, 1999). Eight subtypes of metabotropic glutamate receptors have been cloned so far. They are classified in three groups according to their sequence similarities, transduction mechanisms, and pharmacological profiles (Pin et al., 1999; Schoepp et al., 1999). Group I is composed of $mGlu_1R$ and $mGlu_5R$ that both stimulate PLC hydrolysis. Group II includes $mGlu_2R$ and $mGlu_3R$, which inhibit adenylyl cyclase, as do $mGlu_4R$, $mGlu_6R$, $mGlu_7R$, and $mGlu_8R$ from Group III.

As mentioned above, agonists bind within the large amino terminal extracellular domain (ATD) of these receptors (O'Hara et al., 1993; Takahashi et al., 1993; Okamoto et al., 1998; Hampson et al., 1999; Han & Hampson, 1999). Identifying the structure of this binding domain and the conformational changes resulting from agonist binding would shed some light on the activation mechanism of these receptors. In 1993, O'Hara et al. proposed that mGluR ATDs share structural similarity with bacterial periplasmic amino acid-binding proteins (PBP), such as the leucine-binding protein (LBP) and the leucine/isoleucine/valine-binding protein (LIVBP), the structures of which have been solved by X-ray crys-

Reprint requests to: Francine Acher, Laboratoire de Chimie et Biochimie Pharmacologiques et Toxicologiques, UMR8601-CNRS, Université René Descartes-Paris V, 45 rue des Saints-Pères, 75270 Paris Cedex 06, France; e-mail: acher@biomedicale.univ-paris5.fr.

tallography (O'Hara et al., 1993). This proposal was based on a low sequence identity (17% between LIVBP and mGlu$_1$R ATD) and the mutagenesis of critical binding residues. Since then, the structures of LIVBP and LBP have been used for the generation of tridimensional models of mGluR (Costantino & Pelliciari, 1996; Costantino et al., 1999; Hampson et al., 1999), GABA$_B$ (Galvez et al., 1999), and calcium-sensing (Ray et al., 1999) receptor ATDs, and some of these models have been partially validated by mutagenesis experiments (O'Hara et al., 1993; Bräuner-Osborne et al., 1999; Galvez et al., 1999; Hampson et al., 1999). Structural similarity was also detected between ionotropic glutamate receptor (iGluR) ligand-binding region and the lysine/arginine/ornithine-binding protein (LAOBP), the histidine-binding protein (HBP), and the glutamine-binding protein (QBP), which all belong to a PBP structural cluster different from the one of LIVBP/LBP (Tam & Saier, 1993; Stern-Bach et al., 1994; Lampiden et al., 1998; Felder et al., 1999). This observation was later confirmed by the crystal structure of the ligand-binding core of a GluR subunit (GluR2) in complex with an agonist (Armstrong et al., 1998). However, similarities between iGluRs and mGluRs at both secondary structure and binding site levels are too low to allow the use of this crystal structure as a template.

Periplasmic binding proteins serve as high-affinity active transport of various nutrients such as sugars, inorganic anions, and amino acids. Many of these proteins have been crystallized with and without their ligands and their structures solved by X-ray (Quiocho & Ledvina, 1996). They are all constituted of two globular domains linked by a hinge region and can be found either in an open unliganded, an open liganded, or a closed liganded form (Quiocho & Ledvina, 1996). Accordingly, it has been proposed that the substrate binds to a first lobe and then stabilizes the closed form of the protein.

To support a similar mechanism for family 3 GPCR ATDs, we have investigated the possible three-dimensional (3D)-structures of mGlu$_4$R ATD taken as a representative member of this receptor family and using computational methods. Our aim was to generate a homology-derived model for the open and closed forms of the ATD, and then to analyze the models in terms of their agreement with site-directed mutagenesis, pharmacological profiles, and pharmacophore models (Bessis et al., 1999; Jullian et al., 1999). Our results highlight some new putative residues for each lobe that could interact with the agonist. Altogether, our data support the hypothesis that the agonist is bound to a closed form of the ATD, suggesting this state corresponds to the active state of the receptor.

Results and discussion

Template searching

In 1993, O'Hara et al. proposed that mGluR ATDs share structural similarity with PBP such as LBP and LIVBP. To identify new possible structural templates for mGlu$_4$R ATD, we performed new searches against an updated version of the protein data banks (PDB). We first carried out a classical sequence similarity search using Fasta3 (Pearson & Lipman, 1988). The following results were obtained when using a Blosum62 matrix. LIVBP (PDB code: 2liv) and LBP (PDB code: 2lbp) were recognized as the best templates since matching residues were found all along the query sequence and thus give rise to a subsequent global alignment. Other proposed templates (isomerase 2chs, chorismate mutase 1com, . . .) were not considered since they only match on a short part of the query sequence (42 amino acids overlap or less) and as a result, do not allow a global alignment with matching secondary structure elements (see below). Interestingly, a Blosum 50 retrieved only LIVBP and LBP, whereas a Blosum 75 retrieved 2chs, 1com but not LIVBP and LBP. Yet, sequence identity with mGlu$_4$R ATD was low (19%), as previously observed (O'Hara et al., 1993). Such a low sequence identity between the query sequence and the remote homologues falls in the so-called twilight zone, thus we carried out Psi-Blast (Altschul et al., 1997) and Seqfold (Fisher & Eisenberg, 1996) searches to increase the sensitivity and to support the significance of the initial results. These methods, which take into account not only the sequence but respectively sequence profiles and/or secondary structure predictions, retrieved again LIVBP and LBP with the lowest E-values. AmiC (acetamide-binding protein, PDB code: 1pea) was next retrieved with a lower but acceptable significance. Other hits were not considered since they displayed a much lower significance. Interestingly, AmiC belongs to the same structural cluster as LIVBP and LBP. Indeed, while AmiC shares only 12% sequence identity with LIVBP and LBP, these three proteins belong to the same family of the periplasmic binding protein-like according to the SCOP classification and to the same cluster within this structural family (Tam & Saier, 1993; Chamberlain et al., 1997). LIVBP, LBP, and AmiC are bilobate proteins likely adopting open and closed structures along their activation mechanism. Although LIVBP and LBP have been shown to undergo closure upon ligand binding (Olah et al., 1993), only the structures of their open forms have been solved (Sack et al., 1989a, 1989b). However, a model for a closed state has been proposed, but is not publicly available (Olah et al., 1993). Conversely AmiC has only been crystallized in a closed state (Pearl et al., 1994). Accordingly, the available 3D structures of LIVBP and LBP can be used to construct a 3D model of mGlu$_4$R ATD in a putative open form, whereas the structure of AmiC may constitute a valuable template for a possible closed form.

Alignment

The LIVBP, LBP, AmiC, mGlu$_1$R, mGlu$_2$R, and mGlu$_4$R sequence alignment, generated as described in Materials and methods, is displayed in Figure 1. Other mGluR sequences are not shown since the mGluR family alignment is similar to literature data (Duvoisin et al., 1995). The alignment was further confirmed by the good correspondence between X-ray and predicted secondary structure elements of LIVBP and mGluRs (Fig. 1). Inspection of the secondary structure of mGluRs reveals that some strands (β_B, β_D, β_E, β_a, and β_M identified in LIVBP and LBP) were not predicted. LIVBP α_a and α_b homologous helices were also not predicted for mGluRs. However, they were not predicted when LIVBP sequence was submitted to PHD (data not shown). They were also not depicted in the initial X-ray structure (Sack et al., 1989a). Gaps into LIVBP or LBP secondary structure elements were avoided, except for α_{IX} helix to maintain the alignment of conserved residues on both sides of the gap. This insertion reflects a distortion into the mGluRs' α_{IX} helices allowing a proper orientation of hydrophobic residues, thus improving the structural quality of the model. Yet, the secondary structure homology between LIVBP and mGlu$_4$R ATD reaches 58% compared to 19% sequence identity according to the alignment in Figure 1. This percentage results from the comparison of the number of residues involved in secondary structure elements of LIVBP (β-strands and α-helices, Fig. 1) to the

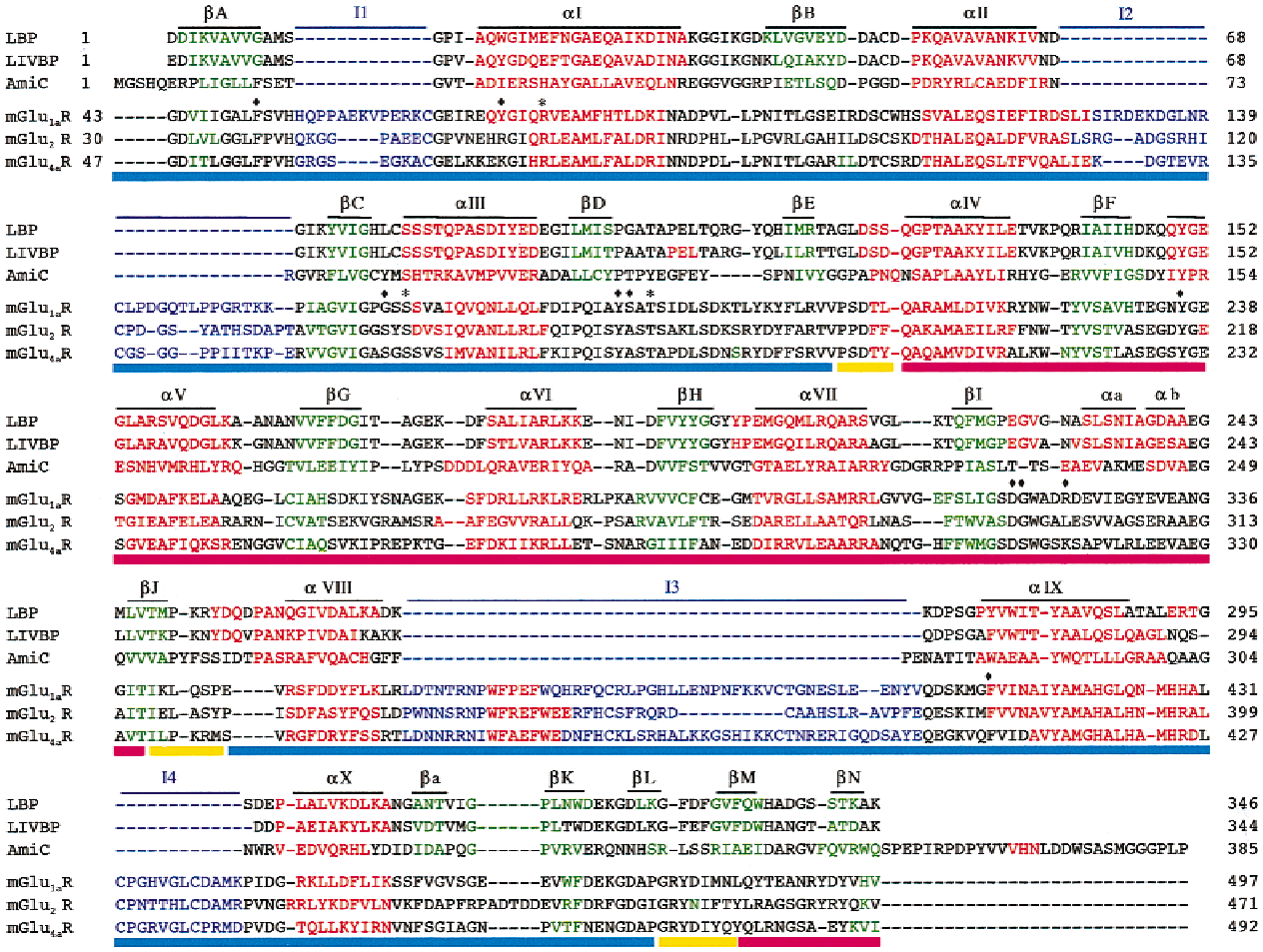

Fig. 1. Sequence alignment of $mGlu_{1,2,4}R$ ATD with LIVBP, LBP, and AmiC. α-Helices (red) and β-strands (green) of LIVBP, LBP, and AmiC are data from PDBSum (http://www.biochem.ucl.ac.uk/bsm/pdbsum). They were named according to Sack et al. (1989a) except for α_a, α_b, and β_a, which were not depicted in this X-ray structure. Secondary structure elements of mGluRs were predicted on PHD (see Materials and methods). Insertions ($I_1 - I_4$) of mGluRs compared to LIVBP or LBP are shown in blue. Residues from lobe I (cyan), lobe II (magenta), and linkers (yellow) are identified with a strip of respective colors. Arg78, Ser159, and Thr182 ($mGlu_4R$), shown to be critical for agonist binding, are marked with (*); other putative binding residues are marked with ♦.

number of residues involved in analogous predicted secondary structure elements of $mGlu_4R$ ATD (Fig. 1). This result supports the hypothesis of a structural homology between the two classes of proteins, although a very low sequence identity was displayed. The final alignment is close to the one previously published by O'Hara et al. (1993), but different from an alternative one proposed by Costantino et al. (1999). It shows four major insertions for $mGlu_4R$ (I_1 amino acids 59–67, I_2 126–148, I_3 353–401, I_4 428–439, Fig. 1) compared to LIVBP and LBP sequences. To avoid the large insertions, Costantino et al. (1999) suggested a different alignment but it does not optimally align secondary structure elements and the resulting model does not agree with recent mutagenesis results (see below). Conversely, the present alignment displays conserved binding residues Arg, Ser, and Thr at positions 78, 159, and 182. Concerning AmiC, a pairwise sequence alignment with LIVBP and LBP was impossible due to the low sequence identity. As a result, this alignment was structurally deduced as described in Materials and methods. Interestingly, the conserved Ser and Thr residues mentioned above are found aligned.

Open form model

On the basis of the sequence alignment with LBP and LIVBP, we constructed a 3D model for the open form of the $mGlu_4R$ ATD. The X-ray structure of the LIVBP template is shown in Figure 2A. It reveals a binding site located within a cleft defined by two lobes (Fig. 2A). The $mGlu_4R$ ATD open model based on LIVBP and LBP coordinates is displayed in Figure 2C. Using an iterative approach (see Materials and methods), we obtained a model with a satisfactory Profiles_3D score (Fig. 3C) that compares favorably to the LIVBP one (Fig. 3A). Only one misfold (defined as a region with a negative Profiles_3D score) with no effect on the putative binding site was observed (Fig. 2C). According to MODELER's probability density functions (PDF), no violations were observed and only few residues (<2%) were located in a disallowed region of the Ramachandran map (data not shown). Insertions I_1 to I_4 are colored in blue (Fig. 1). Two of the four insertions found in $mGlu_4R$ ATD with respect to LIVBP and LBP, namely I_2 (23 amino acids) and I_3 (49 amino acids), had to be respectively truncated from

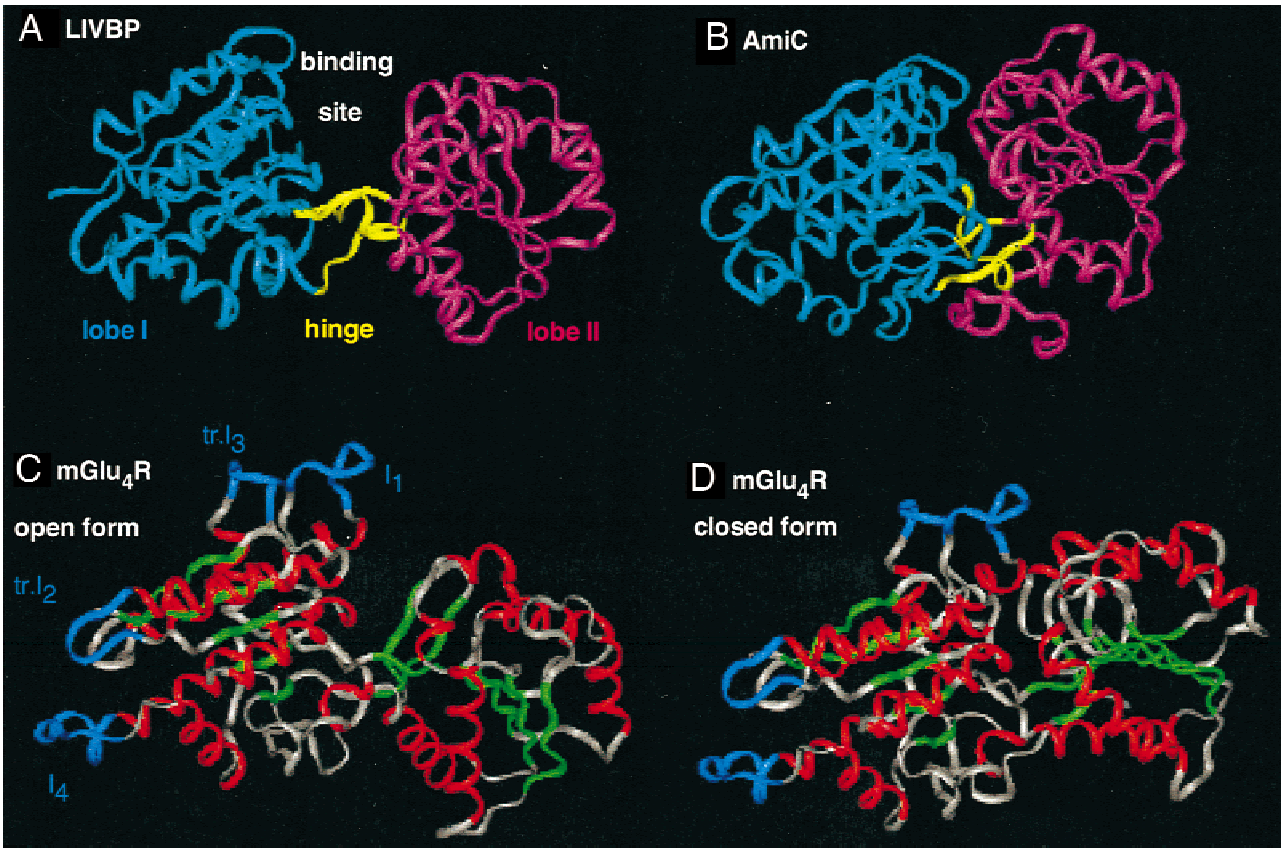

Fig. 2. 3D structures of templates from the PDB: (**A**) LIVBP and (**B**) AmiC. Lobe I, lobe II, and linkers are displayed as a ribbon with similar colors as in Figure 1: cyan, magenta and yellow, respectively. Models of the mGlu$_4$R ATD: (**C**) open form and (**D**) closed form. Insertions I_1 to I_4 are colored in blue (trI indicates truncated insertion), the region (112–114) of negative Profiles_3D score in orange, α-helices in red, and β-strands in green as in Figure 1.

amino acid 132 to 144 and 356 to 397. In fact, all models generated with the large insertions displayed knots between I_2 and I_3 and in their structural core. Accordingly, these insertions were reduced to 7 and 10 amino acids as indicated above, to avoid knots while allowing enough flexibility. Amino acid 124 to 128, at the beginning of I_2, were constrained in the conformation of an α-helix as predicted by PHD (Fig. 1). Since all insertions appear out of the cleft (Fig. 2C), the lack of information on these regions should not affect the topology of the binding site model. Conversely, Arg78, Ser159, and Thr182, which are conserved in all mGluRs and have been shown to be critical for agonist binding (Hampson et al., 1999), are found at the surface of lobe I facing the cleft. On the other hand, Arg106 of mGlu$_1$R, which would be located at the binding site according to Costantino et al.'s (1999) alignment, is not conserved within the mGluRs and aligns with Leu106 of mGlu$_4$R. In the present model it lies outside the cleft on the surface of lobe I.

Agonist pharmacophore models have been established for mGlu$_1$, mGlu$_2$, and mGlu$_4$ receptors, which belong to group I, group II, and group III mGlu receptors, respectively (Bessis et al., 1999; Jullian et al., 1999). They show that in all three cases glutamate would be recognized in an extended conformation. Consequently, the activation by selective Glu-like agonists would result from specific interactions with the different ligand-binding environments and not from the selection of a specific glutamate bioactive conformation. Indeed, each pharmacophore model is characterized by selective sites such as S_4 for mGlu$_4$R (Fig. 4A). A few potent selective agonists are known; they all possess a glutamate embedded in their structure and bind to the protein through the three glutamate common sites S_1 (amino function), S_2 and S_3 (proximal and distal acidic functions) (Fig. 4A) (Bessis et al., 1999; Jullian et al., 1999). The binding of leucine in LIVBP (Sack et al., 1989a) shows that the α-amino and α-acidic groups are bound to Thr102 and Ser79, respectively, and that the hydrophobic side chain interacts with Tyr18. By analogy, Thr182 and Ser159 (mGlu$_4$R), which align with Thr102 and Ser79 (LIVBP), would bind to S_1 and S_2, respectively. The distal site S_3 would interact with Lys74 aligning with Tyr18 of LIVBP (Fig. 1). This ligand binding mode is illustrated with the selective and highly functionalized agonist 1-aminocyclopentane-1,3,4-tricarboxylic acid (ACPT-I) (Acher et al., 1997), which was manually positioned in the open form of mGlu$_4$R ATD (Figs. 4A, left and 4B). Interestingly, Arg78 was found there to interact with the distal function S_3 in agreement with recent mutagenesis experiments (Hampson et al., 1999).

We have previously noted that when agonists are superposed in their bioactive conformations (S_1-S_3 superimposed), all chemical groups generating selectivity were localized on the same face of the superposition (Pin et al., 1999). With S_1-S_3 interaction sites fitted into the open form model, we now observe that most of these selective chemical features (including S_4) are facing lobe II, while

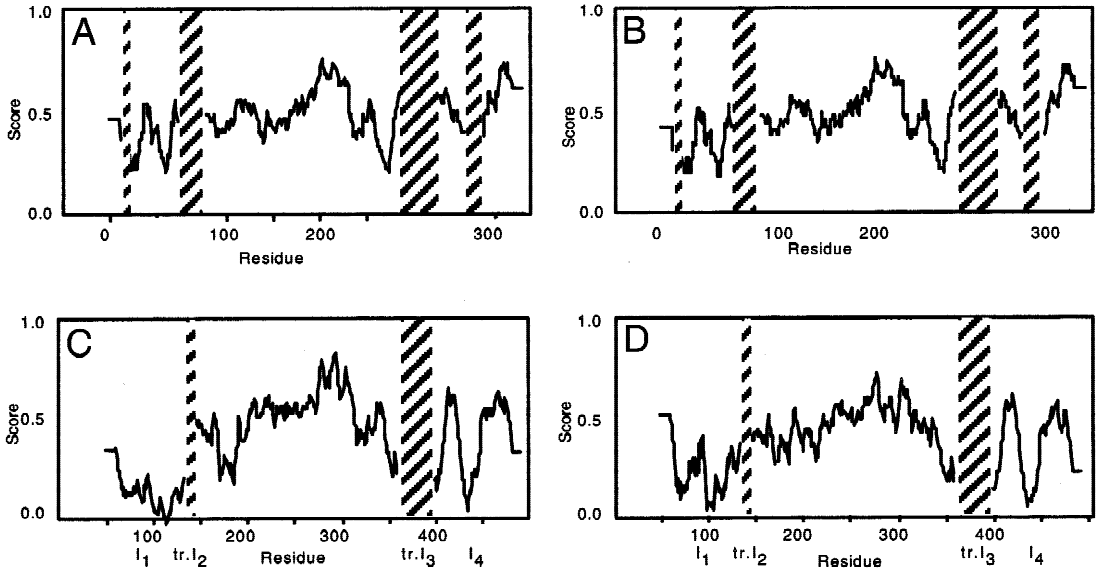

Fig. 3. Profiles_3D plots: (**A**) LIVBP, (**B**) AmiC, (**C**) $mGlu_4R$ ATD open form, and (**D**) closed form.

residues interacting with S_1-S_3 sites (Thr182, Ser159, Lys74, Arg78) are situated on lobe I, as shown for ACPT-I (Fig. 4B). The glutamate entity of ACPT-I, which is mimicked by carbons 1 to 3, lines lobe I while carbon 4 (bearing the selective S_4 function) and carbon 5 are facing lobe II. These observations suggest that lobe II plays an important role in the selectivity of agonist binding in these receptors. In agreement with this proposal, Takahashi et al. (1993) reported that residues 225 to 355 of $mGlu_2R$ were critical in defining the characteristic pharmacological properties of this receptor compared to those of $mGlu_1R$. According to our alignment and 3D models for the ATD of mGluR, these residues constitute the main part of lobe II (Fig. 1). Yet, in our open model, the side chains of the residues of lobe II facing the putative glutamate binding site in lobe I are too distant from the ligand to contact it (Fig. 4B). Therefore, they cannot in the present form be involved in ligand binding selectivity. These observations lead us to generate a model of the closed form of the $mGlu_4R$ ATD to get an insight into additional residues that might bind glutamate and other selective agonists.

Closed form model

Atomic coordinates of LIVBP and LBP closed form are not yet publicly available (Olah et al., 1993; Trakhanov & Quiocho, 1995). However, the closing of the cleft between the two lobes is a general movement for the whole family of PBP (Quiocho & Ledvina, 1996; O'Hara et al., 1999). A hinge-bending motion occurs while the structure of each lobe remains similar. Consequently, only the linker 3D structure of LIVBP or LBP closed form is required to construct the whole $mGlu_4R$ ATD model using structures of the open form lobes. Coordinates of this hinge region were obtained using the structure of the three interdomain segments of AmiC (Fig. 2B) after performing a structure-based alignment with LIVBP. This last alignment was deduced from the superposition of lobe I of LIVBP and AmiC, followed by superposition of lobe II as reported (Pearl et al., 1994). The resulting closed model, which is displayed in Figure 2D, was examined using MODELER's PDF, Profiles_3D score, and Ramachandran maps. Few residues (<2%) were found in the disallowed regions of the Ramachandran map (data not shown), and the Profiles_3D plot (Fig. 3D) is comparable to the LIVBP (Fig. 3A) and AmiC (Fig. 3B) ones. A similar $mGlu_4R$ ATD model was obtained by Hampson et al. (1999). However, these authors did not point out any critical residues belonging to lobe II and involved in agonist binding. To detect such residues, ACPT-I was docked in our closed model and used as a molecular probe, taking advantage of its four functional groups.

Docking of ACPT-I in the closed form model

ACPT-I includes a glutamate structure; therefore, it is likely to bind to the receptor through the three glutamate binding sites S_1-S_3 (see above). It also holds a fourth specific hydrophilic function (S_4, Fig. 4A) (Bessis et al., 1999). ACPT-I was chosen in its putative bioactive conformation as determined in the pharmacophore model. It was manually docked into the binding site of the $mGlu_4R$ ATD closed form model similarly to leucine into LIVBP (Sack et al., 1989a) and L-serin-O-phosphate (L-SOP) into the $mGlu_4R$ ATD model (Hampson et al., 1999): 1-amino group (S_1) in interaction with Thr182, 1-carboxylate (S_2) with Ser159, and 3-carboxylate (S_3) with Lys74 and Arg78. This initial complex was submitted to molecular mechanics and dynamics as described in Materials and methods.

The final model (Figs. 4A, right and 4C) shows that ACPT-I was kept in the same conformation as in the pharmacophore model (Bessis et al., 1999) since the 5-membered ring remained in the same pucker all along the molecular dynamics. Therefore, this result provides a validation of the previous pharmacophore. The present model suggests an important network of interactions involving amino acids of both lobes and anchoring the ligand by all its heteroatoms (Figs. 4C, 5). This model allows us to propose how each of the S_1 to S_4 sites are tied to the protein. The three protons of the amino group (S_1) are respectively bound to the oxygen atom

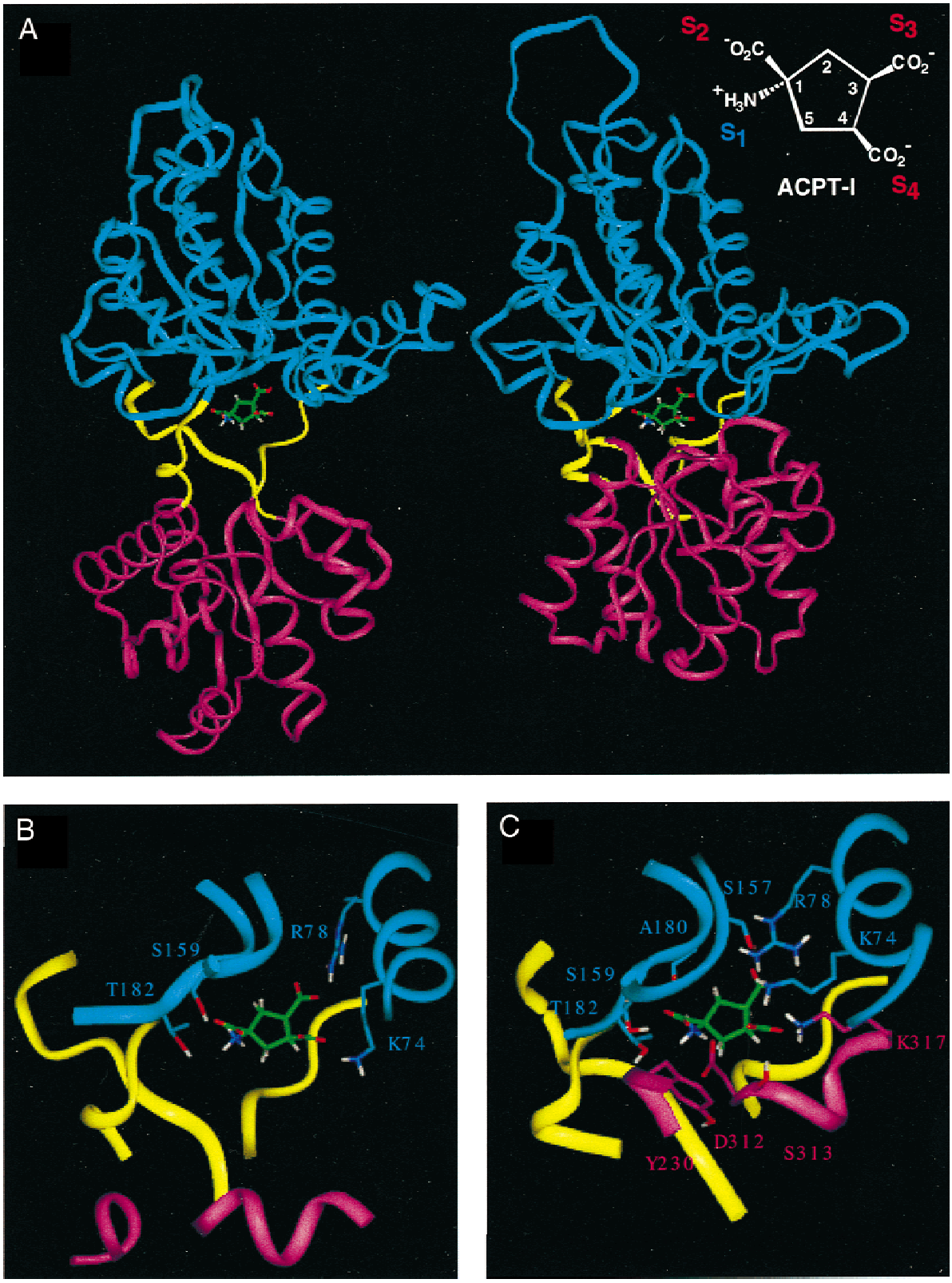

Fig. 4. A: Docking of ACPT-I (carbon atoms in green, nitrogens in blue, oxygens in red) in the mGlu$_4$R ATD models (Cα trace shown, lobes and hinge colored as in Fig. 2A): open form on the left (manual docking), closed form on the right (computational docking). Molecular structure of ACPT-I is shown with S_1 to S_4 binding sites as defined in the pharmacophore model (Bessis et al., 1999) and cyclic carbon atoms numbering. Expanded view of the binding of ACPT-I to the open form model (**B**) and the closed form model (**C**). Side chains of binding residues (experimentally defined (Hampson et al., 1999) or proposed in this study) are displayed in cyan (lobe I) or magenta (lobe II).

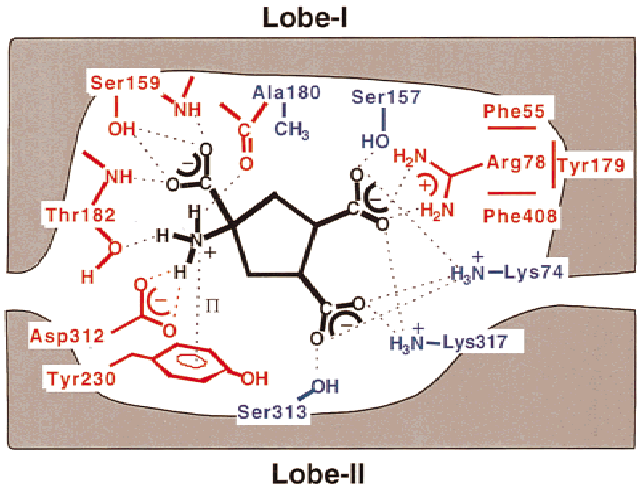

Fig. 5. Synthetic scheme of all interactions observed between ACPT-I and residues from the two lobes (Table 1) of the closed form model of $mGlu_4R$ ATD. Hydrogen bonds are displayed with dashed lines. When interaction occurs between charged functional groups, electrostatic interaction may also take place. A Π symbol indicates the cation Π interaction between the amino group of ACPT-I and Tyr230. The cation Π interactions between Arg78 and the aromatic cluster formed by Phe55, Tyr179, and Phe408 are not materialized for clarity. Residues that are conserved in all mGluRs are in red, those that are either group specific or one receptor type specific are in blue.

of Thr182 side chain, to the oxygen atom of Ala180 backbone, and to the two oxygen atoms of Asp312. Simultaneously, an electrostatic interaction takes place between the positive charge of the ACPT-I amino group and the negative charge of Asp312. Tyr230 contributes to the positioning of the agonist ammonium moiety by means of a cation-Π interaction (Dougherty, 1996; Pullman et al., 1998). The two oxygen atoms of the α-acidic group (S_2) are bound to the hydroxyl side chain of Ser159, one of them to the backbone NH of Ser159, the other one to the backbone NH of Thr182. One of the oxygen atoms of the second acidic group (S_3) is bound to the three ammonium functions of Arg78 and Lys317, the other one to Lys74 ammonium function and to the proton of the hydroxyl group of Ser157. The flexible side chain of Arg78 appears to be well orientated in the binding pocket through cation-Π interactions with three aromatic residues Phe55, Tyr179, and Phe408. The two oxygen atoms of the third acidic group (S_4) are bound to the ammonium function of Lys74; furthermore, one of these atoms is bound to the ammonium function of Lys317 and the other one to the proton of Ser313 hydroxyl (Fig. 5). A stabilizing electrostatic interaction occurs between S_3 and Arg78, Lys317, Lys74 side-chain functions as well as between S_4 and Lys74, Lys317. Carbon 2 of ACPT-I and Ala180 methyl group are in lipophilic interaction, as well as carbon 5 and Tyr230 phenol ring.

While binding to Arg78, Ser159, and Thr182 was expected, the model suggests new bindings to Tyr230 and Asp312, which are conserved in all mGluRs, and to Lys74, Ser157, Ser313, and Lys317, which are subtype or group specific (Table 1). The model also predicts a cluster of aromatic residues (Phe55, Tyr179, Phe408) located around Arg78, which are also conserved in all mGluRs (Table 1). Asp312 and Tyr230 probably play a critical role in anchoring the amino functional group of all mGluRs agonist. Since they are situated on lobe II, they do not contribute to the binding of agonists in the open form, but might play an important role in the activation process. Interestingly, when the glutamyl residue of parathyroid Ca^{2+}-sensing receptor, which aligns with Asp312 of $mGlu_4R$, is mutated, altered calcium homeostasis has been described (Brown & Hebert, 1997). This observation also supports the putative critical role of this residue.

Lys74, Arg78, Lys317, Ser157, and Ser313 form an important basic and hydrophilic cluster that can strongly bind the two distal

Table 1. *Residues[a] involved in the binding of ACPT-I to $mGlu_4R$ ATD and homologous residues[b] from other mGluRs according to the alignment of Figure 1 and known mGluR alignment (Duvoisin et al., 1995)*

	Group III				Group II			Group I	
Lobe	$mGlu_4$	$mGlu_6$	$mGlu_7$	$mGlu_8$	$mGlu_2$	$mGlu_3$	DmGluA	$mGlu_1$	$mGlu_5$
I	Phe55■	—	—	—	—	—	—	—	—
	Lys74	Gln	Asn	—	Arg	Arg	Arg	Tyr	Tyr
	Arg78	—	—	—	—	—	—	—	—
	Ser157	—	—	Ala	—	—	—	Gly	Gly
	Ser159	—	—	—	—	—	—	—	—
	Tyr179■	—	—	—	—	—	Pro	—	—
	Ala180	—	—	—	—	—	—	Ser	Ser
	Thr182	—	—	—	—	—	—	—	—
	Phe408■	—	—	—	—	—	—	—	—
II	**Tyr230**	—	—	—	—	—	—	—	—
	Asp312	—	—	—	—	—	—	—	—
	Ser313□	—	—	—	Gly	Gly	Gly	Gly	Gly
	Lys317□	—	—	—	Leu	Gln	Gln	Arg	Arg

[a] In bold are residues identified as directly contacting the carboxylic or amino group of glutamate, with (■) are residues identified as likely stabilizing the side chain of Arg78 and those labeled with a (□) are residues contacting ACPT-I and which are group III selective.

[b] Residues identical to those of $mGlu_4R$ are indicated with —.

acidic functions of ACPT-I (S_3 and S_4 sites) and may also explain the specific binding of phosphonic ligands as L-AP4 (2-amino-4-phosphono butyric acid) on group-III mGluRs. Among these residues, which are shared between the two lobes (Table 1; Fig. 5), only Arg78 is common to all mGluRs. Consequently, only Lys74, Ser157, Ser313, and Lys317 could eventually explain ACPT-I selectivity. It can be noted that Ser313 and Lys317, which belong to lobe II, are conserved in group III, as it is not the case for Lys74 and Ser157 from lobe I (Table 1). No clear data on the involvement of Lys74 in the activation process are yet available, but two types of results indicate that Ser157 does not play an essential role in agonist binding nor in selectivity. While an alanine residue is found in mGlu$_8$R in place of Ser157 in mGlu$_4$R, ACPT-I affords similar potency on both receptors (De Colle et al., 2000). Furthermore, when this residue (Ser157) was mutated to alanine, hardly any effect was noted on agonist binding (Hampson et al., 1999). We suggest that the role of Ser157 in agonist binding is reduced because of the strong ionic interactions taking place between the distal acidic function S_3 and the three basic residues Lys74, Arg78, and Lys317. According to Hampson's model, the Ser157 side-chain hydroxyl would bind to Arg78, providing a stabilization of this important residue. However, Arg78 would be already positioned by an aromatic cluster (see above) and binding to Ser157 would not be essential. Future studies using new probes or mutants will clarify the role of the binding site residues.

Altogether, ACPT-I, which is trapped in the domain interface, binds to amino acids coming from both lobes and, as such, may contribute to the stabilization of a closed form of mGlu$_4$R ATD, as described for acetamide bound to AmiC (Pearl et al., 1994).

Assuming a common activation mechanism for mGluRs, LIVBP, and AmiC, the selected templates determined the magnitude of the mGlu$_4$R ATD hinge motion, which is ~35° (Chamberlain et al., 1997). However, the amplitude of the rotation of the two domains appears to be quite variable among the family members. While PBPs exhibit a large domain movement, with the amide sensor protein AmiC a small relative hinge motion was detected (Chamberlain et al., 1997; O'Hara et al., 1999). Thus, while the inter-subdomain hinge angle seems to be optimal for ACPT-I bound to the mGlu$_4$R ATD in a closed form model, we have no experimental data to attest to the accuracy of the angle of the open liganded or unliganded form. In fact, this conformation may not be stable since we suppose that an equilibrium occurs between the open and closed conformations with and without a bound ligand, and that activation would be induced by the closed-liganded form (Costantino et al., 1999; Galvez et al., 1999), in agreement with recent data obtained on the GABA-B1 receptor (Galvez et al., 2000). To obtain the best model of this latter form, we had to start with the generation of a bound open form, because of the choice of the LIVBP template. Obviously this first model could not account for the specific interactions of several agonists such as ACPT-I, while it was the case with the closed form allowing interaction of the agonist functional groups with both lobes.

Ultimately, the results of this study support the initial hypothesis that mGluR ATD would close upon ligand binding similarly to PBP.

Materials and methods

Template searching

To identify remote structural homologues, mGlu$_4$R ATD (amino acids 1 to 492 from *Rattus norvegicus* mGlu$_4$R, SwissProt accession number P31423) was used as a query sequence to search structural data banks (e.g., Brookaven Protein Data Bank, SCOP Library). This was done according to various methods: Fasta3, Psi-Blast, Seqfold, based on different techniques: sequence, sequence profile similarities, secondary structure prediction. The PDB was first searched using the Fasta3 method (Pearson & Lipman, 1988) available at the EBI server (http://www.ebi.ac.uk./fasta3) using the default parameters and different blosum scoring matrices. We then performed a Psi-Blast run (Altschul et al., 1997) using a standalone version. The sequence profile was built by searching the SwissProt Data Bank with a Blosum62 matrix. The converged profile was subsequently utilized to search the PDB. We performed as well a Seqfold search (Fisher & Eisenberg, 1996) (InsightII version 2000, Molecular Simulations Inc., San Diego, California). Seqfold gives the ability to search against a fold library (e.g., SCOP, http://www.scop.mrc-lmb.cam.ac.uk/scop) using either a DSC secondary structure prediction (King & Sternberg, 1996) alone or in combination with the Psi-Blast profile.

Sequence alignment

To get an optimal sequence alignment between mGlu$_4$R ATD and LIVBP and LBP, we proceeded in three steps. A ClustalW (version 1.6) (Thompson et al., 1994) multiple sequence alignment was first performed using the sequences of metabotropic glutamate receptor ATD (rat mGlu$_{1\text{-}8}$R plus the *Drosophila* receptor DmGlu$_A$R), Ca^{2+}-sensing receptor ATD, LIVBP, and LBP. A Blosum30 was used as a scoring matrix; gap penalties and extension gap penalties were set to 30 and 0.05, respectively. The alignment was then manually modified to avoid gaps into secondary structure elements. For LIVBP and LBP, secondary structures were considered according to various methods: crystallographic data (PDB Sum, http://www.biochem.ucl.ac.uk/bsm/pdbsum), Kabsch and Sander algorithm (InsightII version 980, MSI), and secondary structure predictions (Rost & Sander, 1993) using PHD (http://www.maple.bioc.columbia.edu/predictprotein/). For mGlu$_4$R ATD, only the PHD prediction could be used. The resulting alignment was then used to generate 3D models of the mGlu$_4$R ATD open form that were evaluated as described below. The alignment was further iteratively modified to increase the structural quality of our model. The alignment of AmiC with LIVBP and LBP was deduced from the structural superposition of each lobe of the closed form of AmiC on the corresponding lobe of the open form of LIVBP (Pearl et al., 1994).

Open and closed models of mGlu$_4$R ATD (AA47–492)

Both mGlu$_4$R ATD models (open and closed forms) were generated by the automated homology modeling tool MODELER 5.00 (InsightII version 980, MSI) (Sali & Blundell, 1990). The 3D open form model was generated using the coordinates of LIVBP and LBP open forms from *Escherichia coli* deposited at the PDB. The sequence alignment used was obtained as described above. Then the quality of each model generated by MODELER was evaluated with different independent criteria. Invalid models with important structural violations, especially knots, were eliminated thanks to the PDF of MODELER. The remaining models were then submitted to the Profiles_3D algorithm using a sequence window of 21 amino acids (Profiles_3D, InsightII version 980, MSI)(Luthy et al., 1992). This algorithm calculates the compatibility between a given sequence of amino acids, and its associated modeled structures and

helps to identify misfolded regions. This statistical tool allowed us to locally modify the sequence alignment and to generate iteratively new models until we reached an optimal score equivalent to 96% of theoretical score. The best resulting open model as well as its Profiles_3D score are displayed in Figures 2C and 3C. The corresponding final alignment (Fig. 1) was retained to generate a 3D closed model of $mGlu_4R$ ATD with truncated I_2 an I_3 insertions, as described above. This model was constructed using the coordinates of the two lobes of LIVBP (Lobe I: amino acids 1–118, 253–325; Lobe II: amino acids 125–247, 332–344) and LBP (Lobe I: amino acids 1–118, 253–327; Lobe II: amino acids 125–247, 334–346) crystalline open forms, the coordinates of the two lobes of the open form model of $mGlu_4R$ ATD (Lobe I: amino acids 47–199, 341–470; Lobe II: amino acids 206–334, 480–492), and the coordinates of the three linkers (amino acids 121–129, 252–264, 335–344) of the hinge region of AmiC crystalline closed form. The best resulting model as well as its Profiles_3D are displayed in Figures 2D and 3D.

Docking of ACPT-I in the putative binding site of $mGlu_4R$ ATD closed form

ACPT-I (Fig. 3A) was chosen with protonated amino group and deprotonated carboxylic groups, while a neutral pH ionization state was set for the residue side chains. ACPT-I, in the conformation of the agonist $mGlu_4R$ pharmacophore model, was initially manually docked in $mGlu_4R$ ATD closed form, in agreement with the position of L-leucine in the LIVBP active site. The ammonium and the α-carboxylate functions were facing Thr182 and Ser159, respectively, while one of the two distal acidic functions was pointing toward Lys74 to let the second one point to the lobe II. The ligand-protein complex was submitted to energy minimization using Steepest Descent (until derivative less than 2 kcal/mol/Å) and Conjugated Gradient (until derivative less than 0.01 kcal/mol/Å) while Cα_trace was tethered using a quadratic potential. This was performed using the Discover 3.00 calculation engine with the CFF force field (InsightII version 980, MSI). The nonbond cut-off method and the dielectric constant were set up to cell multipole and distance-dependent, respectively ($\epsilon = r$). Discover 3.00 and CFF force field were further used to perform a molecular dynamics at 298 K on the previously minimized system. The tethering force on Cα trace was successively decreased by reducing the force constant value of the quadratic potential from 100 to 60, 30, 20, 10, and 0 every 40 ps. The molecular dynamics was then continued during 240 ps. The integration time step was set up to 1 fs, and the calculations were performed at constant volume and temperature. A snapshot of the system was saved every 400 fs. Once the system was equilibrated, the coordinates of 20 snapshots were averaged and submitted again to the previously described minimization protocol with no Cα restraints. Contacts between the ligand and the protein were subsequently analyzed using the web interface of the WHATIF program (http://www.swift.embl-heidelberg.de/servers2).

Acknowledgments

This work was supported by grants from the CNRS (PCV97-115) and RETINA France. The authors wish to thank Parke-Davis Pharmaceutical Research (Ann Arbor, Michigan) for allowing a Fulbright scholarship to A.-S. Bessis, and G. Milioti, N. Jullian, K. Olswezski, B. Hartmann for suggestions and critical reading of the manuscript.

References

Acher F, Tellier F, Brabet I, Fagni L, Azerad R, Pin J-P. 1997. Synthesis and pharmacological characterization of aminocyclopentane tricarboxylic acids (ACPT): New tools to discriminate between metabotropic glutamate receptor subtypes. *J Med Chem 40*:3119–3129.

Altschul SF, Madden TL, Schaffer AA, Zhang J, Zhang Z, Miller W, Lipman DJ. 1997. Gapped BLAST and PSI-BLAST: A new generation of protein database search programs. *Nucleic Acids Res 25*:3389–3402.

Armstrong N, Sun Y, Chen G-Q, Gouaux E. 1998. Structure of a glutamate-receptor ligand-binding core in complex with kainate. *Nature 395*:913–917.

Bessis A-S, Jullian N, Coudert E, Pin J-P, Acher F. 1999. Extended glutamate activates metabotropic receptor types 1, 2 and 4: Selective features at mGluR4 binding site. *Neuropharmacology 38*:1543–1551.

Bockaert J, Pin J-P. 1999. Molecular tinkering of G-protein coupled receptors: An evolutionary success. *EMBO J 18*:1723–1729.

Bräuner-Osborne H, Jensen AA, Sheppard PO, O'Hara P, Krogsgaard-Larsen P. 1999. The agonist-binding domain of the calcium-sensing receptor is located at the amino-terminal domain. *J Biol Chem 274*:18382–18386.

Brown EM, Hebert SC. 1997. Calcium-receptor-regulated parathyroid and renal function. *Bone 20*:303–309.

Chamberlain D, O'Hara BP, Wilson SA, Pearl LH, Perkins SJ. 1997. Oligomerization of the amide sensor protein AmiC by X-ray and neutron scattering and molecular modeling. *Biochemistry 36*:8020–8029.

Conn PJ, Pin J-P. 1997. Pharmacology and functions of metabotropic glutamate receptors. *Ann Rev Pharmacol Toxicol 37*:205–237.

Costantino G, Macchiarulo A, Pellicciari R. 1999. Modeling of amino-terminal domains of group I metabotropic glutamate receptors: Structural motifs affecting ligand selectivity. *J Med Chem 42*:5390–5401.

Costantino G, Pelliciari R. 1996. Homology modeling of metabotropic glutamate receptors (mGluRs). Structural motifs affecting binding modes and pharmacological profile of mGluR1 agonists and competitive antagonists. *J Med Chem 39*:3998–4006.

De Colle C, Bessis A-S, Bockaert J, Acher F, Pin J-P. 2000. Pharmacological characterization of the rat metabotropic glutamate receptor type 8a revealed strong similarities and slight differences with the type 4a receptor. *Eur J Pharmacol 394*:17–26.

Dougherty DA. 1996. Cation-II interaction in chemistry and biology: A new view of benzene, Phe, Tyr, and Trp. *Science 271*:163–167.

Duvoisin RM, Zhang CX, Ramonell K. 1995. A novel metabotropic glutamate receptor expressed in the retina and olfactory bulb. *J Neurosci 15*:3075–3083.

Felder CB, Graul RC, Lee AY, Merkle H-P, Sadée W. 1999. The venus flytrap of periplasmic binding proteins: An ancient protein module present in multiple drug receptors. *AAPS Pharmsci*. www.pharmsci.org

Fisher D, Eisenberg D. 1996. Protein fold recognition using sequence-derived predictions. *Protein Sci 5*:947–955.

Galvez T, Parmentier M-L, Joly C, Malitschek B, Kaupmann K, Kuhn R, Bittiger H, Froestl W, Bettler B, Pin J-P. 1999. Mutagenesis and modeling of the GABAb receptor extracellular domain support a venus flytrap mechanism for ligand binding. *J Biol Chem 274*:13362–13369.

Galvez T, Prézeau L, Milioti G, Franek M, Joly C, Froestl W, Bettler B, Bertrand H-O, Blahos J, Pin J-P. 2000. Mapping the agonist binding site of GABAB type 1 subunit sheds light on the activation process of GABAB receptors. *J Biol Chem*. Forthcoming.

Gomeza J, Joly C, Kuhn R, Knöpfel T, Bockaert J, Pin J-P. 1996. The second intracellular loop of metabotropic glutamate receptor 1 cooperates with the other intracellular domains to control coupling to G-proteins. *J Biol Chem 271*:2199–2205.

Hampson DR, Huang X-P, Pekhletski R, Peltekova V, Hornby G, Thomsen C, Thøgersen H. 1999. Probing the ligand-binding domain of the mGluR4 subtype of metabotropic glutamate receptor. *J Biol Chem 274*:33488–33495.

Han G, Hampson DR. 1999. Ligand binding to the amino-terminal domain of the mGluR4 subtype of metabotropic glutamate receptor. *J Biol Chem 274*:10008–10013.

Jullian N, Brabet I, Pin J-P, Acher F. 1999. Agonist selectivity of mGluR1 and mGluR2 metabotropic receptors: A different environment but similar recognition of an extended glutamate conformation. *J Med Chem 42*:1546–1555.

King RD, Sternberg MJE. 1996. Identification and application of the concepts important for accurate and reliable protein secondary structure prediction. *Protein Sci 5*:2298–2310.

Lampiden M, Pentikäinen O, Johnson MS, Keinänen K. 1998. AMPA receptors and bacterial periplasmic amino acid-binding proteins share the ionic mechanism of ligand recognition. *EMBO J 17*:4704–4711.

Luthy R, Bowie JU, Eisenberg D. 1992. Assessment of protein models with three-dimensional profiles. *Nature 356*:83–85.

O'Hara BP, Norman RA, Wan PT, Roe SM, Barrett TE, Drew RE, Pearl LH. 1999. Crystal structure and induction mechanism of AmiC-AmiR: A ligand-regulated transcription antitermination complex. *EMBO J 18*:5175–5186.

O'Hara PJ, Sheppard PO, Thogersen H, Venezia D, Haldeman BA, Mc Grane V, Houamed KH, Thomsen C, Gilbert TL, Mulvihill ER. 1993. The ligand-binding domain in metabotropic glutamate receptors is related to bacterial periplasmic binding proteins. *Neuron 11*:41–52.

Okamoto T, Sekiyama N, Otsu M, Shimada Y, Sato A, Nakanishi S, Jingami H. 1998. Expression and purification of the extracellular ligand binding region of metabotropic glutamate receptor subtype 1. *J Biol Chem 273*:13089–13096.

Olah GA, Trakhanov S, Trewhella J, Quiocho FA. 1993. Leucine/isoleucine/valine-binding protein contracts upon binding of ligand. *J Biol Chem 268*: 16241–16247.

Pearl L, O'Hara B, Drew R, Wilson S. 1994. Crystal structure of AmiC: The controller of transcription antitermination in the amidase operon of *Pseudomonas aeruginosa*. *EMBO J 13*:5810–5817.

Pearson WR, Lipman DJ. 1988. Improved tools for biological sequence analysis. *Proc Natl Acad Sci USA 85*:2444–2448.

Pin J-P, De Colle C, Bessis A-S, Acher F. 1999. New perspective in the development of selective metabotropic glutamate receptor ligands. *Eur J Pharmacol 375*:277–294.

Pin J-P, Joly C, Heinemann SF, Bockaert J. 1994. Domains involved in the specificity of G protein activation in phospholipase C coupled metabotropic glutamate receptor. *EMBO J 13*:342–348.

Pullman A, Berthier G, Savinelli R. 1998. Interaction of the tetrametylammonium ion with the cycles of aromatic amino acids beyond the SCF ab initio level. *J Am Chem Soc 120*:8553–8554.

Quiocho FA, Ledvina PS. 1996. Atomic structure and specificity of bacterial periplasmic receptors for active transport and chemotaxis: Variation of common themes. *Mol Microbiol 20*:17–25.

Ray K, Hauschild BC, Steinbach PJ, Goldsmith PK, Spiegel AM. 1999. Identification of the cysteine residues in the amino-terminal extracellular domain of the human Ca^{2+} receptor critical for dimerisation. *J Biol Chem 274*: 27642–27650.

Rost B, Sander C. 1993. Prediction of protein secondary structure at better than 70% accuracy. *J Mol Biol 232*:584–599.

Sack JS, Saper MA, Quiocho FA. 1989a. Periplasmic binding protein structure and function. Refined X-ray structures of the leucine/isoleucine/valine-binding protein and its complex with leucine. *J Mol Biol 206*:171–191.

Sack JS, Trakhanov SD, Tsigannik IH, Quiocho FA. 1989b. Structure of the L-leucine-binding protein refined at 2.4 Å resolution and comparison with the Leu/Ile/Val-binding protein structure. *J Mol Biol 206*:193–207.

Sali A, Blundell TL. 1990. Definition of general topological equivalence in protein structures: A procedure involving comparison of properties and relationships through simulated annealing and dynamic programming. *J Mol Biol 212*:403–428.

Schoepp DD, Jane DE, Monn JA. 1999. Pharmacological agents acting at subtypes of metabotropic glutamate receptors. *Neuropharmacology 38*:1431–1476.

Stern-Bach Y, Bettler B, Hartley M, Sheppard PO, O'Hara P, Heinemann SF. 1994. Agonist selectivity of glutamate receptors is specified by two domains structurally related to bacterial amino acid-binding proteins. *Neuron 13*: 1345–1357.

Takahashi K, Tsuchida K, Tanabe Y, Masu M, Nakanishi S. 1993. Role of the large extracellular domain of metabotropic glutamate receptors in agonist selectivity determination. *J Biol Chem 268*:19341–19345.

Tam R, Saier MHJ. 1993. Structural, functional, and evolutionary relationships among extracellular solute-binding receptors of bacteria. *Microbiol Rev 57*:320–346.

Thompson JD, Higgins DG, Gibson TJ. 1994. CLUSTAL W: Improving the sensitivity of progressive multiple sequence alignment through sequence weighting, positions-specific gap penalties and weight matrix choice. *Nucleic Acids Res 22*:4673–4680.

Trakhanov S, Quiocho FA. 1995. Influence of divalent cations in protein crystallization. *Protein Sci 4*:1914–1919.